Thymine dissociation and dimer formation: A Raman and synchronous fluorescence spectroscopic study

Anushka Nagpal[a] , Dinesh Dhankhar[a] , Thomas C. Cesario[b] , Runze Li[a] , Jie Chen[c] , and Peter M. Rentzepis[a,1]

[a]Department of Electrical and Computer Engineering, Texas A&M University, College Station, TX 77843; [b]School of Medicine, University of California, Irvine, CA 92697; and [c]School of Physics and Astronomy, Shanghai Jiao Tong University, 200240 Shanghai, China

In this study, absorption, fluorescence, synchronous fluorescence, and Raman spectra of nonirradiated and ultraviolet (UV)-irradiated thymine solutions were recorded in order to detect thymine dimer formation. The thymine dimer formation, as a function of irradiation dose, was determined by Raman spectroscopy. In addition, the formation of a mutagenic (6-4) photoproduct was identified by its synchronous fluorescence spectrum. Our spectroscopic data suggest that the rate of conversion of thymine to thymine dimer decreases after 20 min of UV irradiation, owing to the formation of an equilibrium between the thymine dimers and monomers. However, the formation of the (6-4) photoproduct continued to increase with UV irradiation. In addition, the Raman spectra of nonirradiated and irradiated calf thymus DNA were recorded, and the formation of thymine dimers was detected. The spectroscopic data presented make it possible to determine the mechanism of thymine dimer formation, which is known to be responsible for the inhibition of DNA replication that causes bacteria inactivation.

thymine dimer | DNA | spectroscopy | thymine dimer Raman spectrum | UV inactivation

In the United States alone, each year 2.8 million antibiotic-resistant infections occur that cause about 35,000 deaths (1). Such resistant organisms are often acquired in the hospital (2) and may well be from contaminated surfaces (3). Ultraviolet (UV) light has become a critical means to control some of these antibiotic-resistant organisms and to prevent them from infecting vulnerable patients (4). Therefore, improving our understanding of the microbiologic effects of UV light has become more important. Further, UV light also has an antimicrobial effect on the RNA of viruses, including coronaviruses (5), which further increases our need to understand the chemical basis for the biological effects of UV light. DNA damage, such as deamination, oxidative damage, strand breaks, and dimer formation, can hinder normal functioning of a cell, prevent DNA replication, and cause cell death (6). UV-induced DNA damage results mainly in damage to pyrimidine bases, thus inducing the formation of cyclobutane pyrimidine dimers (CPDs), pyrimidine(6-4)pyrimidone photoproducts, and Dewar isomers (7). It is widely believed, but not previously shown spectroscopically, that inactivation of bacteria by UV irradiation is caused by the dissociation of the double bond of the thymine base of the bacterial DNA followed by the formation of a single bond formed between two adjacent thymine bases, which results in the formation of thymine CPDs (8). These dimers dissociate the hydrogen bonds between bases of complementary DNA strands and consequently inhibit the replication of DNA (9, 10). It has been reported that the most abundant photoproduct formed after UV irradiation is the thymine dimer T-T, followed by thymine cytosine dimer T-C, thymine cytosine (6-4) photoproduct T(6-4)C, and thymine (6-4) photoproduct T(6-4)T (11, 12). Many studies have suggested that the thymine (6-4) photoproduct is as mutagenic as the thymine CPD (13, 14); however, the (6-4) photoproduct is formed with a smaller yield (12). Fig. 1A shows the structure of thymine, thymine CPD, and (6-4) photoproduct (15). Minor UV photoproducts include cytosine dimers (C-C), cytosine

thymine dimers (C-T), and their respective (6-4) adducts, which are formed in much smaller quantities (12).

Purine bases are considered to be virtually immune to UV light. The formation of adenine dimers and adenine thymine photoproducts has also been observed; however, their yield is orders of magnitude smaller than that of the pyrimidine dimers and their adducts (16, 17).

Previous studies have proposed that the thymine CPD, in frozen thymine solutions, is formed by the combination of the excited singlet state of the thymine monomers (18), whereas the (6-4) photoproduct is formed from an oxetane intermediate (7). As a result, thymine dimers can dissociate and reconvert into thymine monomers by UV irradiation. However, we find, in accordance with previous studies, that the (6-4) photoproducts are not converted to thymine monomers by UV irradiation (13). When the (6-4) photoproduct is irradiated with 313-nm light it is reversibly converted to another UV photoproduct, known as Dewar isomer, which converts back to the (6-4) photoproduct upon irradiation with 240-nm light (19).

Spectroscopic analysis of bacteria provides a fast and cost-effective method for the determination of bacterial strains and, in addition, allows for the detection of live and dead bacteria after UV irradiation (20, 21). In our study, aqueous solutions of thymine and DNA were irradiated with UV light and changes in their Raman spectra were compared, before and after irradiation, in order to detect UV-induced photoproducts. Aqueous thymine solutions were frozen at 240 K and then irradiated with 254-nm UV light. The absorption spectrum of thymine is shown in Fig. 1B. When aqueous thymine solution is frozen, water molecules start to crystallize into a hexagonal structure in order to attain the lowest energy configuration. The water crystallization process

Significance

Bacteria inactivation by ultraviolet light is caused due to the formation of thymine dimers that inhibit DNA replication. We have used spectroscopic means for the identification of thymine dimer(s) that may pave the way for fast and definite identification of the ratio of live and dead bacteria, as suggested by our previous spectroscopic studies. In the present study, the dissociation of thymine to thymine dimers and (6-4) photoproducts was detected by means of a Raman, absorption, and synchronous fluorescence study. These data provide a fast method for determining, in situ, the reaction mechanism and final photoproducts formed as a function of UV irradiation dose.
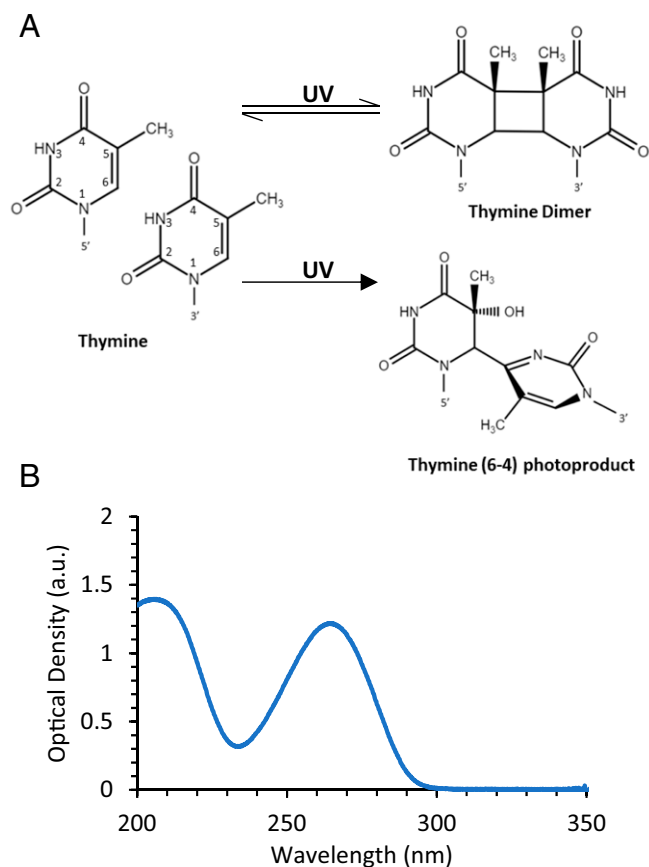
Fig. 1. (A) Structure of thymine, thymine dimer (CPD), and (6-4) photoproduct. (B) Absorption spectrum of thymine solution.

(ice formation) excludes thymine molecules and consequently leads to separation of the solvent and solute components (22). Therefore, as the water crystallizes, the thymine solution becomes more concentrated and crystallizes into thymine monohydrate crystals (23). The preferred structural orientation of these crystals is such that the thymine monomers are stacked on top of each other, yielding the perfect structural orientation for dimer formation. This arrangement of the frozen thymine monomers mimics the arrangement of the thymine monomers in DNA strands, which also form thymine dimers upon UV irradiation at room temperature (24).

In agreement with previous studies (25, 26), our experiments show that when thymine solution is irradiated with UV light the absorption band intensity at 260 nm decreases due to the dissociation of the thymine monomers and the formation of photoproducts. The thymine dimer, in contrast to the thymine monomer, does not absorb at 260 nm, because the 260-nm absorbing C=C is converted to C–C, while the (6-4) photoproduct exhibits an absorption maximum at 315 nm. To confirm the formation of thymine dimers, after UV irradiation at 240 K we reirradiated the irradiated solution at 300 K. We observed (Fig. 2) that the absorption band at 260 nm increases with thymine irradiation time at room temperature, owing to the dissociation of thymine dimers and their conversion to thymine monomers.

Thymine solution exhibits a weak fluorescence with maximum intensity at 325 nm, when excited at 260 nm (27), and upon UV irradiation with 254-nm light at 240 K the thymine fluorescence decreases. We also observed that the (6-4) photoproduct fluoresces with a maximum at 375 nm, when excited at 315 nm, whereas no thymine dimer fluorescence was observed. Therefore, to detect thymine dimers which were not previously identified

spectroscopically we recorded the Raman spectra of thymine before and after irradiation.

Raman spectroscopy is a well-known powerful method for the study of biological molecules, including amino acids, proteins, nucleic acids, lipids, and other molecules (28–33). This fast and noninvasive technique, based on the inelastic scattering of monochromatic light from a molecule, provides a structural fingerprint by recording their vibrational and rotational transitions. As a result, it is widely used for structural analysis and the identification of molecules.

Results

Irradiation of Thymine Solution.

Absorption spectra. The absorption spectra of thymine solution before and after irradiation for 5, 10, 20, 30, and 60 min are shown in Fig. 3A. This figure shows that, upon irradiation with 0.66 mW/cm^2 UV light, the maximum intensity at 263.8 nm, which is assigned to thymine monomer, decreases as a function of irradiation time.

Thymine dimers exhibit weak absorption at wavelengths longer than 220 nm, whereas the (6-4) photoproduct absorbs at 315 nm. The decrease in optical density (OD) at 260 nm as a function of irradiation dose is shown in Fig. 4.

Examination of Figs. 3 and 4 shows that the (6-4) photoproduct band increases with irradiation time; however, the decrease of the thymine monomer spectral intensity, at 260 nm, does not follow the same trend. The OD at 260 nm decreases from OD = 1.2, before irradiation, to OD = 0.2, after 10 min of irradiation, and remains constant at OD~0.13 for 60 irradiation minutes. We assign the OD plateau to thymine dimers' dissociation and reconversion to thymine monomers. Prolonged UV irradiation results in an equilibrium, established between the thymine monomer and dimer, that is evidenced by the plateau of OD vs. irradiation time, shown in Fig. 4. In contrast, the (6-4) photoproducts do not convert back to thymine monomer, and hence their concentration continues to increase as a function of irradiation dose.
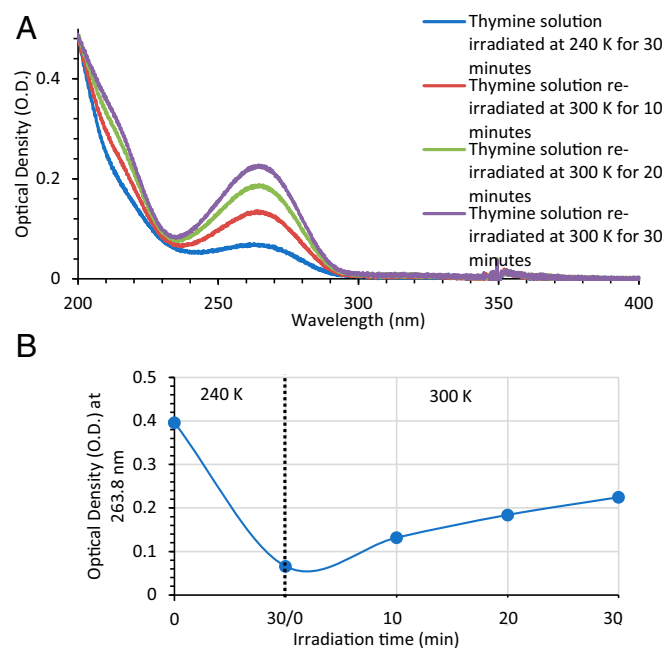

Fig. 2. (A) Absorption spectrum of thymine solution irradiated with 254-nm light at 240 K and reirradiated at 300 K for 10, 20, and 30 min. (B) Change in OD at 263.8 nm, after UV irradiation at 240 K followed by irradiation at 300 K, as a function of irradiation time (minutes).
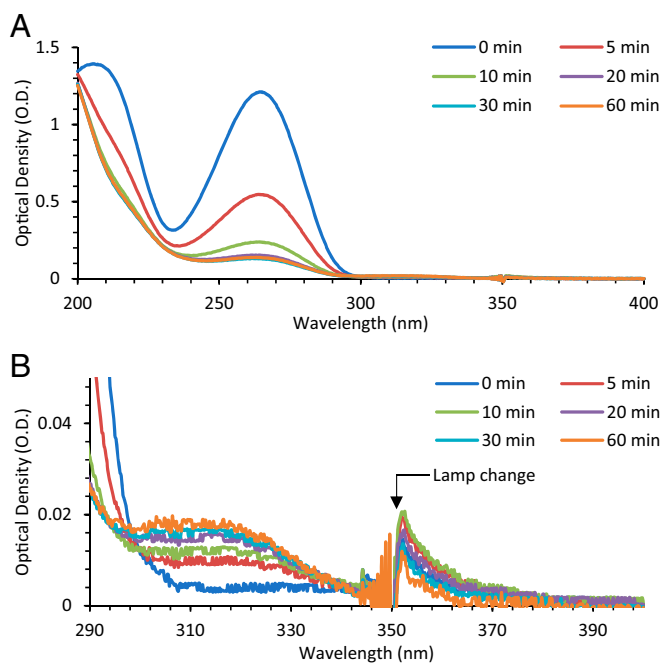
Fig. 3. Absorption spectrum of thymine solution irradiated with 254-nm UV light for 0, 5, 10, 20, 30, and 60 min. (*A*) Decrease in OD as a function of irradiation dose. (*B*) Same spectrum at OD interval 0 to 0.05. The band at 355 nm is due to the Hg lamp change intensity.

Fluorescence spectra. Aqueous thymine solution exhibits a weak fluorescence, with a maximum at 325 nm, when excited at 260 nm (Fig. 5). When this solution is irradiated with 254-nm light, at 240 K for 10 min, the 325-nm thymine fluorescence maximum decreases and a new band with maximum at 375 nm is detected, which we assign to the formation of the (6-4) photoproduct (34). A much stronger fluorescence band of this photoproduct is emitted when the irradiated solution of thymine is excited at 315 nm, where the absorption band has its maximum.

A lower concentration, 5.267×10^{-5} M, was selected for recording these spectra because irradiation of higher concentrations results in the formation of higher concentrations of (6-4) photoproduct, whose intense fluorescence masks the fluorescence emitted by thymine monomers. As a result, the decrease in thymine fluorescence is not clearly observed when a higher concentration of thymine solution is irradiated.

The fluorescence emission spectra of the nonirradiated and irradiated thymine solutions, excited at 315 nm, are shown in Fig. 6*A*. A new band at 375 nm is recorded, which corresponds to the fluorescence maximum of the (6-4) photoproduct (34) that increases with irradiation dose.

UV irradiation of thymine solution results in the increase of the fluorescence band intensity at 375 nm and also in increase of the absorption intensity at 315 nm (Fig. 6*B*). From these data, we conclude that the (6-4) photoproduct concentration increases with irradiation dose. We also observed that while the (6-4) photoproduct has an intense fluorescence spectrum the thymine dimer does not emit any detectable fluorescence. This is due to the presence of conjugation in (6-4) photoproducts and its absence in thymine dimers.

The synchronous fluorescence spectra of the nonirradiated and irradiated thymine solutions are shown in Fig. 7*A*, where $\Delta\lambda = 50$ nm. The band with maximum at 369 nm is assigned to the (6-4) photoproduct. Fig. 7*B* shows the increase in intensity at 369 nm as a function of irradiation dose, which follows the same trend as the fluorescence emission; this validates further the 369-nm fluorescence band assignment to (6-4) photoproducts.
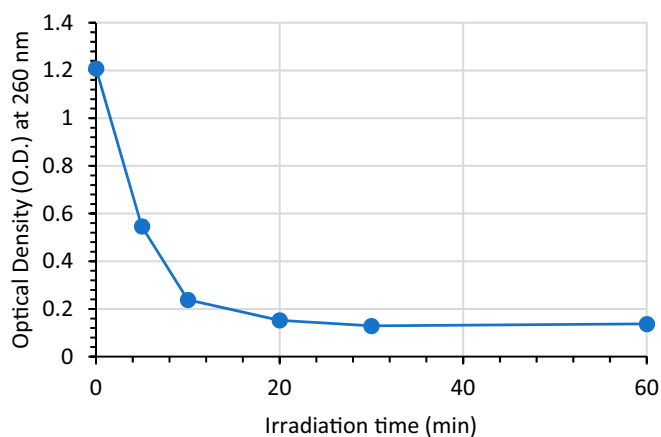

Fig. 4. Decrease in OD of thymine solution at 263.8 nm as a function of irradiation time (minutes).

Raman spectra. The maximum at 1,666 cm^{-1} in the Raman spectra of the unirradiated thymine solution (Fig. 8*A*) is assigned to $C_4=O$ and $C_5=C_6$ stretching vibrations (35–37). When thymine is irradiated, this peak shifts to 1,687 cm^{-1} (Fig. 8*B*). This shift occurs because the $C_5=C_6$ bond of the thymine monomer dissociates, when irradiated, to form a single C–C bond with an adjacent thymine monomer, thus forming a thymine dimer. As a result, the stretching mode of the $C_4=O$ bond shifts toward longer wavenumbers, as the π electrons localize and strengthen this bond. Fig. 9 shows the change in the ratio of the maximum intensities at 1,687 cm^{-1} to 1,666 cm^{-1} as a function of irradiation time, where the red dots represent the ratio of the intensities at 1,687 cm^{-1} to 1,666 cm^{-1} for each spectrum recorded and the blue line represents the average of the aforementioned ratios for each irradiation time interval.

Fig. 9 shows clearly that thymine converts to the dimer during the first 20 min of irradiation and then remains constant, suggesting that the thymine dimer dissociates and converts back to the monomer(s). As a result, an equilibrium is established between the dimers and monomers.

The maximum, at 1,361 cm^{-1}, in the Raman spectrum of thymine solution is assigned to the symmetric deformation (umbrella bending) of the CH_3 group connected with an sp^2 hybridized carbon atom (C_5 atom in this case) (35, 37). When thymine monomer is irradiated, the band intensity maximum decreases with irradiation time, as is clearly depicted in Fig. 8. This occurs
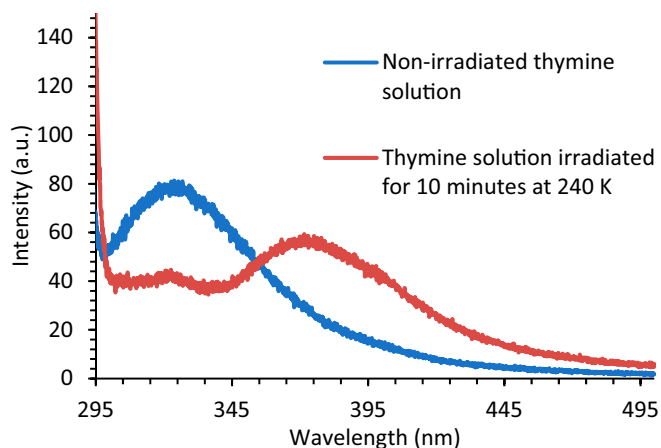

Fig. 5. Fluorescence emission spectra of nonirradiated and irradiated thymine solutions excited at 260 nm.
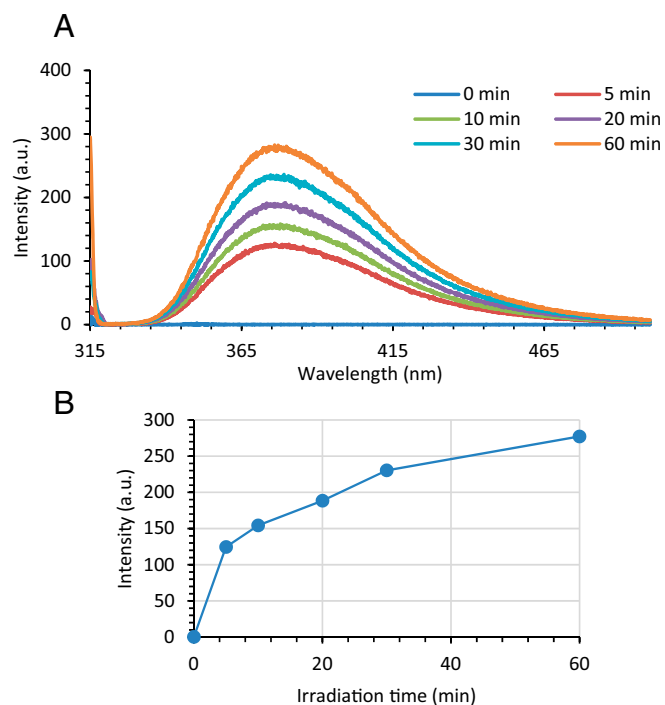
Fig. 6. (*A*) Fluorescence emission spectra of nonirradiated and irradiated thymine solutions excited at 315 nm. (*B*) Change in fluorescence intensity at 375 nm with irradiation time (minutes).
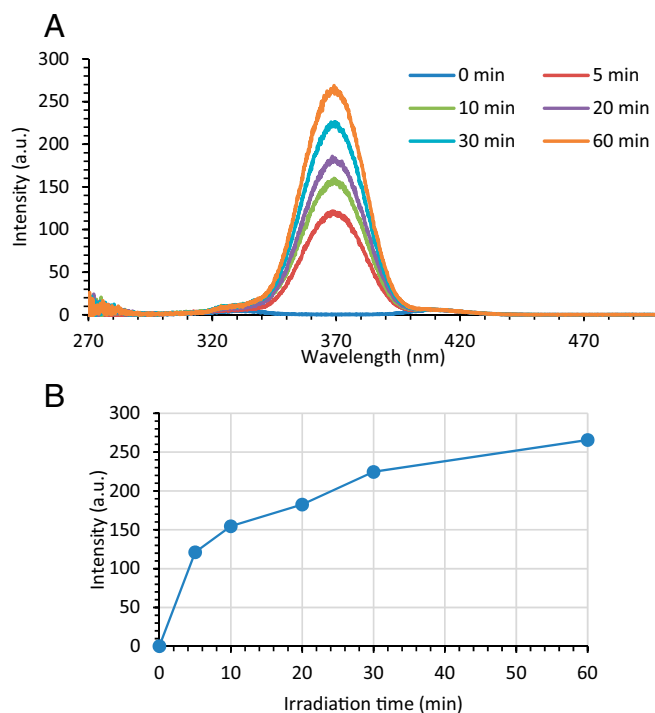

Fig. 7. (*A*) Synchronous fluorescence spectra of nonirradiated and irradiated thymine solutions, $\Delta\lambda = 50$ nm. (*B*) Increase in the synchronous fluorescence intensity at 369 nm as a function of irradiation time.

because, upon irradiation of thymine monomers, the $C_5{=}C_6$ bond dissociates and therefore the CH_3 group is no longer bonded to an sp^2 hybridized carbon but to an sp^3 hybridized carbon.

The Raman scattering intensity of the bending frequency of the CH_3 group, bonded to an sp^3 carbon atom, is known to be very weak, and therefore it is often not observed by Raman spectroscopy. This occurs because the polarizability of the CH_3 group decreases owing to the loss of π electrons as the $C_5{=}C_6$ bond dissociates to form $C_5{-}C_6$. The change in the ratio of the maximum intensities of the bonds at 1,687 cm^{-1} to 1,361 cm^{-1} as a function of irradiation time is shown in Fig. 10, where the red dots represent the ratio of the intensities at 1,687 cm^{-1} to 1,361 cm^{-1} for each spectrum recorded and the blue line represents the average of the aforementioned ratios for each irradiation time interval.

The differences observed in the Raman bands of the thymine monomer and dimer in the 2,850 cm^{-1} to 3,200 cm^{-1} spectral region yield information concerning the mechanism of formation of a thymine dimer by the combination of two monomers. It is therefore necessary to assign the spectral band maxima in this region to the corresponding bond vibrations. Fig. 11*A* shows the Raman spectrum of thymine monomer: The broad maximum at 3,000 cm^{-1} and the maximum at 2,966 cm^{-1} are assigned to the asymmetric C–H stretch of the CH_3 group; the intense band at 2,933 cm^{-1} and weak peak at 2,896 cm^{-1} are assigned to the symmetric C–H stretching of the CH_3 group and the maximum at 3,068 cm^{-1} to C_6H stretch vibration (36, 37).

The C–H stretch is located at 2,850 cm^{-1} to 2,990 cm^{-1} when the C is sp^3 hybridized, at 3,000 cm^{-1} to 3,100 cm^{-1} when the C is sp^2 hybridized, and at 3,300 cm^{-1} when the C is sp hybridized. This occurs because, as the bond strength increases, the stretching frequency also increases. When the thymine monomer converts to a dimer, the hybridization of the C_6 atom changes from sp^2 to sp^3, due to the dissociation of the $C_5{=}C_6$ bond. Fig. 11*A* shows that the C_6–H stretch in the Raman spectrum of the unirradiated thymine solution is located at 3,068 cm^{-1} because C_6 is sp^2 hybridized. As

thymine is irradiated, the $C_5{=}C_6$ bond dissociates and forms a C–C bond with another similarly dissociated $C_5{=}C_6$ bond of an adjacent thymine monomer, forming the thymine dimer. As a
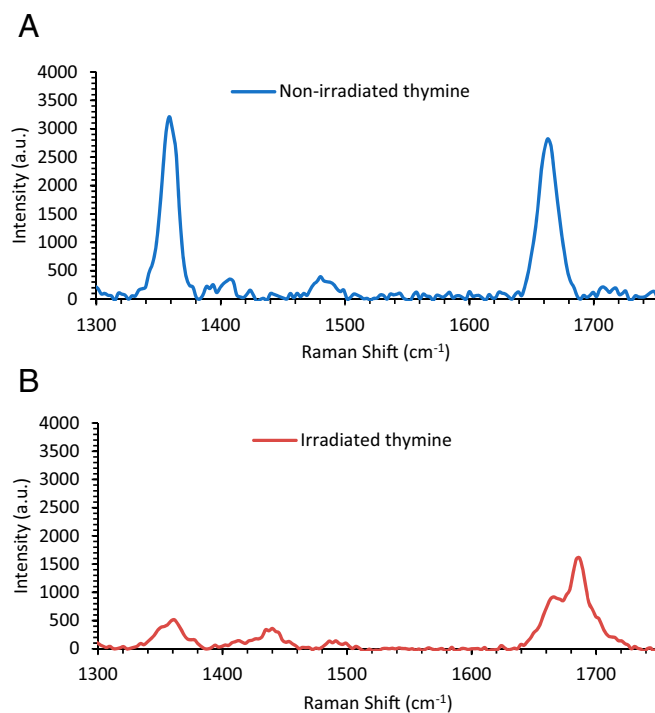

Fig. 8. Raman spectra, after baseline subtraction, in the 1,300 cm^{-1} to 1,750 cm^{-1} region of (*A*) nonirradiated thymine and (*B*) thymine irradiated with 254-nm UV light for 10 min.
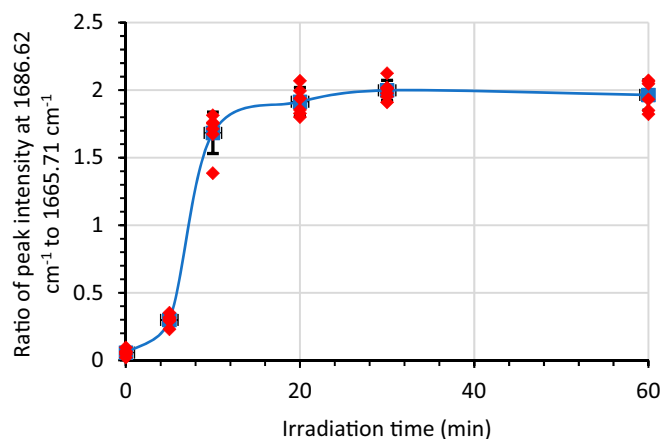
Fig. 9. Change in ratio of the peak Raman intensities of thymine at 1,687 cm^{-1} to 1,666 cm^{-1} as a function of irradiation time (minutes).

Fig. 10. Change in ratio of the peak Raman intensities of thymine at 1,687 cm^{-1} to 1,361 cm^{-1} as a function of irradiation time (minutes).

result, the C$_6$ becomes sp^3 hybridized, and the maximum at 3,068 cm^{-1} is expected to shift below 3,000 cm^{-1}, owing to dimer formation. To that effect, we observed that with UV irradiation the band with maximum at 3,068 cm^{-1} vanishes and a new band with maxima at 2,986 cm^{-1} appears. This intense and broad band is a superimposition of several vibrational bands (Fig. 11*B*).

Previous studies have reported the presence of a weak maximum, at 1,246 cm^{-1}, in the Raman spectrum of thymine solution, which was assigned to the ring-stretching vibration of thymine (35, 37). We have recorded the same maximum in the Raman spectrum of DNA which is assigned to thymine ring-stretching vibration. In order to observe this maximum, we used the 100× objective to record the Raman spectrum.

Fig. 12 shows the Raman spectra of the unirradiated and irradiated thymine solution recorded using the 100× objective. The maximum at 1,246 cm^{-1} begins to decrease in intensity after UV irradiation and vanishes after 10 min of continuous irradiation. A similar decrease is also observed when DNA solution is irradiated, as discussed later in this paper.

Irradiation of DNA Solution. The Raman spectra of nonirradiated and UV-irradiated DNA solutions are shown in Fig. 13. The maximum at 1,375 cm^{-1} in the Raman spectra of the unirradiated DNA solution (Fig. 8*A*) is assigned to Raman vibrational bands of thymine, adenine, and guanine. When DNA solution is irradiated a decrease in this band is observed (Fig. 8*B*). A similar decrease at 1,361 cm^{-1} was also detected in the Raman spectrum of the UV-irradiated thymine solution. The decrease in this band in DNA can, therefore, be attributed to the dissociation of the thymine base, as the UV irradiation-induced purine photoproducts are shown to be several orders of magnitude smaller than thymine photoproducts (16, 17).

Fig. 14 shows the change in the maximum intensity at 1,375 cm^{-1} as a function of irradiation time, where the red dots represent the intensity at 1,375 cm^{-1} for each spectrum recorded and the blue line displays the average of the aforementioned intensities for each irradiation time interval. It is evident that the decrease in the maximum at 1,375 cm^{-1} follows the same trend observed in the thymine solution.

The maximum at 1,248 cm^{-1} in the Raman spectra of the unirradiated DNA solution (Fig. 8) is assigned to the Raman vibration of thymine (38, 39). The same band observed in the Raman spectrum of thymine is assigned to the ring-stretching vibration of thymine. As DNA is irradiated with UV light thymine photoproducts are formed whose formation alters the ring-stretching vibration and causes a decrease in the intensity of this band. We observed a similar change in this Raman band when
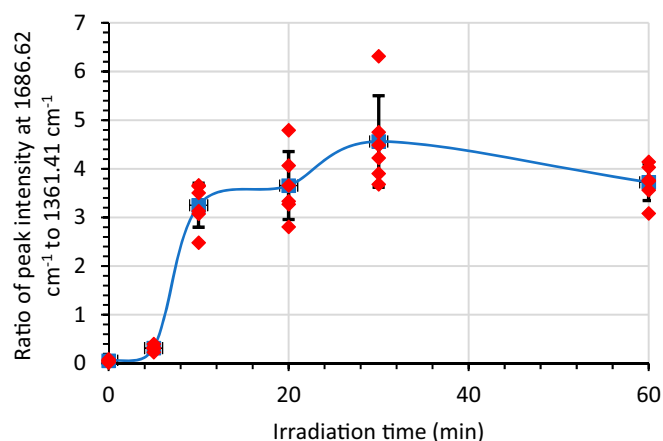
thymine was irradiated in frozen solution: The band at 1,246 cm^{-1} in the Raman spectrum of thymine solution vanishes within 10 min of UV irradiation.

The broad band that we recorded at 1,665 cm^{-1} is due to the superimposition of Raman bands of thymine, cytosine, and guanine, in agreement with ref. 38. We observed a decrease in this Raman band which is similar to that seen in the Raman spectrum of thymine solution after UV irradiation.

Fig. 15 shows the change in the maximum intensity at 1,665 cm^{-1} as a function of irradiation time, where the red dots represent the intensity at 1,665 cm^{-1} for each spectrum recorded and the blue line represents the average of the aforementioned intensities for each irradiation time interval.

It is interesting to note that the changes in the Raman spectra of nonirradiated and irradiated DNA solutions display changes
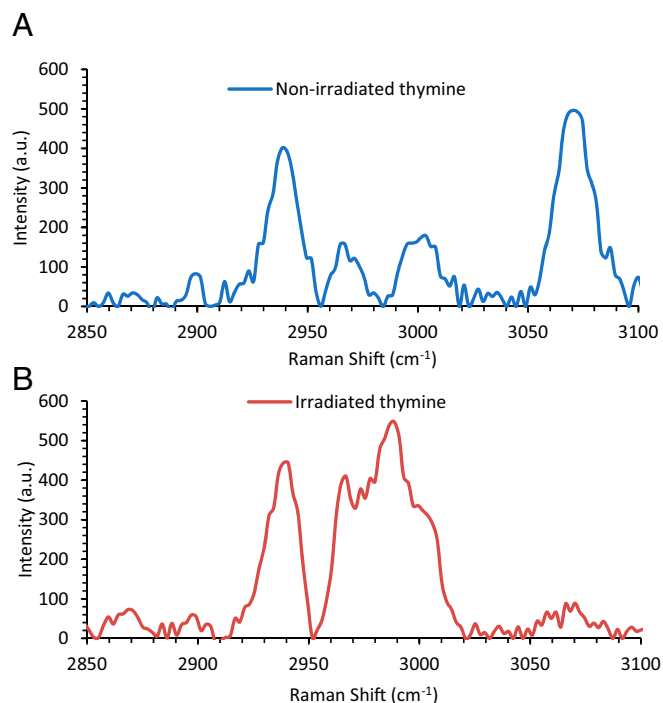
Fig. 11. Raman spectra of (*A*) nonirradiated thymine and (*B*) thymine irradiated with 254-nm light for 10 min in the 2,850 cm^{-1} to 3,100 cm^{-1} region.

Nagpal et al.
Thymine dissociation and dimer formation: A Raman and synchronous fluorescence spectroscopic study
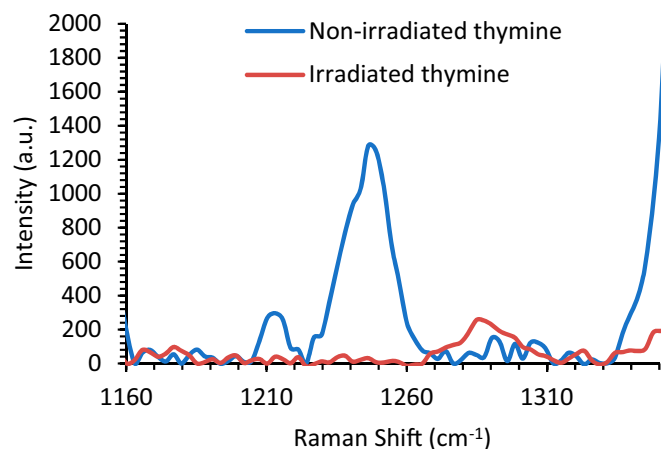
PNAS | 5 of 7
https://doi.org/10.1073/pnas.2025263118

Fig. 12. Change in the thymine Raman maximum intensity at 1,246 cm^{-1}, corresponding to the ring-stretching vibration, on irradiation with 254-nm light.

Fig. 13. Normalized Raman spectra in the 1,150 cm^{-1} to 1,750 cm^{-1} region of nonirradiated DNA (blue) and DNA irradiated for 30 min with 254-nm UV light (red).

similar to those observed in the Raman spectrum of nonirradiated and irradiated thymine solutions. Therefore, we have shown that the formation of thymine photoproducts in DNA can be realized spectroscopically by Raman analysis.

The spectral changes reported in this paper strongly support the mechanism that is proposed for the formation of a C_5–C_6 bond of thymine dimer from the C_5=C_6 bond of the thymine monomer and its subsequent dissociation due to further irradiation. This process is also responsible for the irradiation-induced DNA thymine dimer formation that prohibits DNA replication and subsequently initiates DNA reconstruction with further irradiation owing to dimer dissociation.

Discussion

By means of Raman spectroscopy we have identified the formation of thymine dimers in both thymine and DNA which are crucial for the determination of live and dead bacteria ratio owing to the fact that dimer formation hinders the replication of bacterial DNA (21). In this study, the mechanism of thymine dimer formation and dissociation has been identified by their Raman spectral band changes as a function of irradiation dose. The absorption, fluorescence, and synchronous fluorescence were also recorded and analyzed for nonirradiated and irradiated thymine solutions. Upon UV irradiation, the formation of a new fluorescence band was detected with maximum at 375 nm, which we assigned to (6-4) photoproducts. The fluorescence intensity of these photoproducts increased with irradiation dose, indicating continuous (6-4) photoproduct formation as a function of irradiation dose. We also recorded the Raman spectral bands of the thymine monomer located at 1,666 cm^{-1} and 3,068 cm^{-1} that shift to 1,687 cm^{-1} and 2,986 cm^{-1}, respectively, upon UV irradiation. We find that the thymine monomer Raman bands with a maximum at 1,361 cm^{-1} and 1,246 cm^{-1} decrease and eventually vanish upon continuous UV irradiation. We conclude, therefore, that these changes in the Raman spectra occur due to the formation of thymine dimers. Furthermore, the plot of the ratio of the band intensities as a function of irradiation time shows that the conversion of thymine to dimers and (6-4) photoproducts slows after 20 min of irradiation and begins to saturate owing to the establishment of an equilibrium between thymine monomer and dimer concentration. We also established that this trend is similar to the decrease of the thymine absorption maximum at 263.8 nm. The observed continuous increase of the (6-4) photoproducts is due to the fact that these photoproducts do not convert back to thymine monomer, in contrast to the photo-reversible dimer. Four
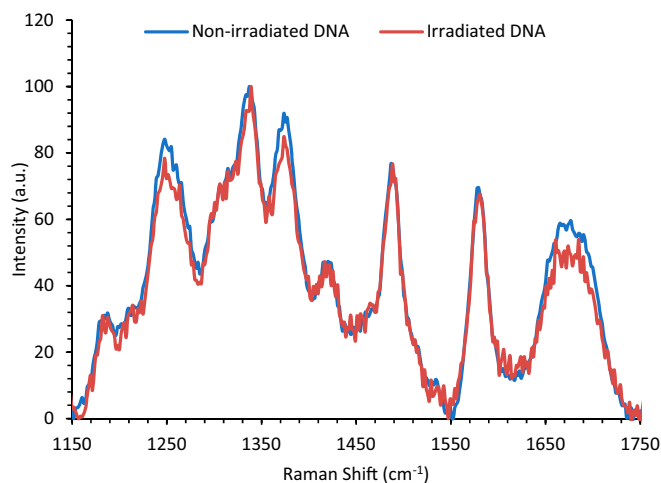
experiments carried out under the same experimental parameters were compared, and the data were found to be identical. We also recorded the Raman spectrum of nonirradiated and irradiated calf thymus DNA and observed that the bands at 1,375 cm^{-1}, 1,248 cm^{-1}, and 1,665 cm^{-1} all decrease in intensity with UV irradiation, which is very similar to that observed in Raman spectrum of UV-irradiated thymine.

Materials and Methods

UV Irradiation of Thymine Solution. One milliliter of aqueous thymine solution, 1.5342×10^{-4} M, at 240 K, was irradiated with 254-nm, 0.66 mW/cm^2 light emitted by an Hg (Ar) pencil lamp. A bandpass UV filter, with 23.82% transmittance at 254 nm, was used to filter out wavelengths other than 254 nm; however, a minimal amount of 302-nm, 312-nm, and 365-nm lines were also transmitted. A quartz lens focused the transmitted light onto the sample. The procedure followed for UV irradiation was as follows: 1 mL of thymine solution was frozen for 10 min then irradiated for time intervals of 5, 10, 20, 30, and 60 min and subsequently allowed to thaw at room temperature for 10 min.

Absorption, Fluorescence, and Raman Spectra of Thymine Solution. The absorption, fluorescence, and Raman spectra were recorded using Shimadzu UV160U spectrophotometer, Shimadzu RF-6000 fluorophotometer, and Horiba XploRA PLUS Raman microscope, respectively. The absorption and
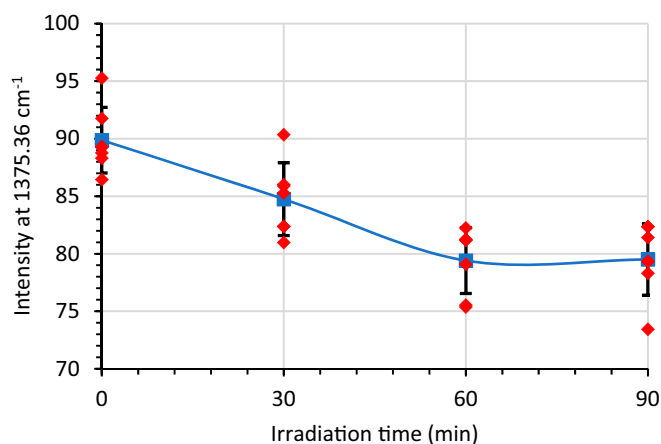

Fig. 14. Change in the Raman intensity of DNA at 1,375 cm^{-1} assigned to the vibrational bands of thymine, adenine, and guanine as a function of irradiation time (minutes).
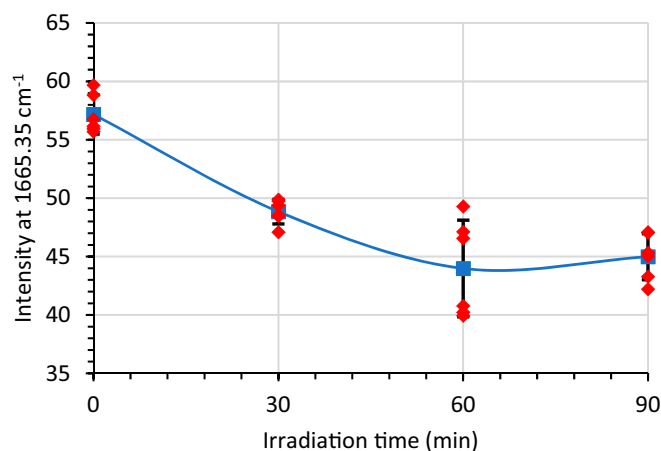
Fig. 15. Change in the Raman intensity of DNA at 1,665 cm^{-1} assigned to the vibrational bands of thymine, guanine, and cytosine as a function of irradiation time (minutes).

fluorescence spectra of nonirradiated and irradiated thymine solutions were recorded for each irradiation period of time and dose. The spectra were recorded at room temperature in a 1-cm optical path length quartz cuvette. The spectral resolution of the absorption measurements was 2 nm and the emission and excitation bandwidths were 3 nm, unless otherwise stated.

A 5-μL drop of the thymine solution was placed on a mirror and dried and subsequently Raman spectra were recorded before irradiation and after each

irradiation dose using a confocal Raman microscope. The Raman spectra recorded were excited by 532-nm laser light, using a 10× objective lens and 1,200 g/mm grating. The resolution of the Raman spectra was 2.7 cm^{-1}. Six Raman spectra were recorded for each irradiation dose and nonirradiated thymine solution. Baseline correction was performed for each spectrum and all spectra were normalized with respect to the 1,666 cm^{-1} spectral region, corresponding to the C=O stretching vibration in thymine, for the purpose of comparing different Raman band maxima.

UV Irradiation of DNA Solution. Calf thymus DNA solution (44.7 μg/mL) was irradiated at room temperature in a 1-cm path length quartz cuvette with 3 mW/cm^2 light emitted by a mercury vapor lamp. A bandpass UV filter with 23.82% transmittance at 254 nm was used to allow only 250- to 380-nm light to be transmitted to a quartz lens, which focused it onto the sample. Three milliliters of aqueous DNA solution was irradiated for 30, 60, and 90 min.

Raman Spectra of DNA Solution. A 20-μL drop of the aqueous DNA solution was placed on a mirror and dried. The Raman spectra were recorded before and after each irradiation dose. The Raman spectra were recorded using a 638-nm laser light, a 100× objective lens, and 1,200 g/mm grating. Six Raman spectra were recorded for the nonirradiated DNA solution and for each irradiation dose. The baseline was corrected and normalized with respect to the 1,335 cm^{-1} Raman band of adenine, which decreases very slightly upon UV irradiation.

1. CDC, Antibiotic resistance threats in the United States, 2019 (US Department of Health and Human Services, CDC, Atlanta, GA, 2019).
2. D. J. Weber, R. Raasch, W. A. Rutala, Nosocomial infections in the ICU: The growing importance of antibiotic-resistant pathogens. *Chest* **115** (suppl.(3), 34S–41S (1999).
3. J. A. Otter, S. Yezli, J. A. Salkeld, G. L. French, Evidence that contaminated surfaces contribute to the transmission of hospital pathogens and an overview of strategies to address contaminated surfaces in hospital settings. *Am. J. Infect. Control* **41** (suppl.(5), S6–S11 (2013).
4. J. M. Boyce, C. J. Donskey, Understanding ultraviolet light surface decontamination in hospital rooms: A primer. *Infect. Control Hosp. Epidemiol.* **40**, 1030–1035 (2019).
5. C. M. Walker, G. Ko, Effect of ultraviolet germicidal irradiation on viral aerosols. *Environ. Sci. Technol.* **41**, 5460–5465 (2007).
6. K. Sofińska, N. Wilkosz, M. Szymoński, E. Lipiec, Molecular spectroscopic markers of DNA damage. *Molecules* **25**, 561 (2020).
7. H. Ikehata, T. Ono, The mechanisms of UV mutagenesis. *J. Radiat. Res. (Tokyo)* **52**, 115–125 (2011).
8. R. Beukers, J. Ijlstra, W. Berends, The effect of ultraviolet light on some components of the nucleic acids. VI the origin of the U.V. sensitivity of deoxyribonucleic acid. *Recl. Trav. Chim. Pays Bas* **79**, 101–104 (1960).
9. R. B. Setlow, J. K. Setlow, Evidence that ultraviolet-induced thymine dimers in DNA cause biological damage. *Proc. Natl. Acad. Sci. U.S.A.* **48**, 1250–1257 (1962).
10. R. B. Setlow, Cyclobutane-type pyrimidine dimers in polynucleotides. *Science* **153**, 379–386 (1966).
11. A. J. Varghese, S. Y. Wang, Thymine-thymine adduct as a photoproduct of thymine. *Science* **160**, 186–187 (1968).
12. T. Douki, J. Cadet, Individual determination of the yield of the main UV-induced dimeric pyrimidine photoproducts in DNA suggests a high mutagenicity of CC photolesions. *Biochemistry* **40**, 2495–2501 (2001).
13. H. Yokoyama, R. Mizutani, Structural biology of DNA (6-4) photoproducts formed by ultraviolet radiation and interactions with their binding proteins. *Int. J. Mol. Sci.* **15**, 20321–20338 (2014).
14. J. E. LeClerc, A. Borden, C. W. Lawrence, The thymine-thymine pyrimidine-pyrimidone(6-4) ultraviolet light photoproduct is highly mutagenic and specifically induces 3′ thymine-to-cytosine transitions in Escherichia coli. *Proc. Natl. Acad. Sci. U.S.A.* **88**, 9685–9689 (1991).
15. J. Li, T. Uchida, T. Todo, T. Kitagawa, Similarities and differences between cyclobutane pyrimidine dimer photolyase and (6-4) photolyase as revealed by resonance Raman spectroscopy: Electron transfer from the FAD cofactor to ultraviolet-damaged DNA. *J. Biol. Chem.* **281**, 25551–25559 (2006).
16. P. H. Clingen, R. J. H. Davies, Quantum yields of adenine photodimerization in poly(deoxyadenylic acid) and DNA. *J. Photochem. Photobiol. B* **38**, 81–87 (1997).
17. S. N. Bose, R. J. Davies, S. K. Sethi, J. A. McCloskey, Formation of an adenine-thymine photoadduct in the deoxydinucleoside monophosphate d(TpA) and in DNA. *Science* **220**, 723–725 (1983).
18. J. Eisinger, R. G. Shulman, The precursor of the thymine dimer in ice. *Proc. Natl. Acad. Sci. U.S.A.* **58**, 895–900 (1967).
19. H. E. Johns, M. L. Pearson, J. C. Leblanc, C. W. Helleiner, The ultraviolet Photochemistry of thymidylyl-(3′-5′)-thymidine. *J. Mol. Biol.* **9**, 503–524 (1964).
20. R. Li, D. Dhankhar, J. Chen, T. C. Cesario, P. M. Rentzepis, A tryptophan synchronous and normal fluorescence study on bacteria inactivation mechanism. *Proc. Natl. Acad. Sci. U.S.A.* **116**, 18822–18826 (2019).
21. R. Li et al., Identification of live and dead bacteria: A Raman spectroscopic study. *IEEE Access* **7**, 23549–23559 (2019).
22. S. Y. Wang, Photochemical reactions in frozen solutions. *Nature* **190**, 690–694 (1961).
23. S. Y. Wang, The mechanism for frozen aqueous solution irradiation of pyrimidines. *Photochem. Photobiol.* **3**, 395–398 (1964).
24. W. Füchtbauer, P. Mazur, Kinetics of the ultraviolet-induced dimerization of thymine in frozen solutions. *Photochem. Photobiol.* **5**, 323–335 (1966).
25. D. L. Wulff, G. Fraenkel, On the nature of thymine photo-product. *Biochim. Biophys. Acta* **51**, 332–339 (1961).
26. R. B. Setlow, W. L. Carrier, Identification of ultraviolet-induced thymine dimers in DNA by absorbance measurements. *Photochem. Photobiol.* **2**, 49–57 (1963).
27. M. A. Morsy, A. M. Al-Somali, A. Suwaiyan, Fluorescence of thymine tautomers at room temperature in aqueous solutions. *J. Phys. Chem. B* **103**, 11205–11210 (1999).
28. J. T. Edsall, J. W. Otvos, A. Rich, Raman spectra of amino acids and related compounds. VII. Glycylglycine, cysteine, cystine and other amino acids1. *J. Am. Chem. Soc.* **72**, 474–477 (1950).
29. D. Garfinkel, Raman spectra of amino acids and related compounds. XII. Various amino acids derived from proteins and creatine1,2. *J. Am. Chem. Soc.* **80**, 3827–3831 (1958).
30. A. Rygula et al., Raman spectroscopy of proteins: A review. *J. Raman Spectrosc.* **44**, 1061–1076 (2013).
31. M. Pézolet, T.-J. Yu, W. L. Peticolas, Resonance and preresonance Raman spectra of nucleotides using ultraviolet lasers. *J. Raman Spectrosc.* **3**, 55–64 (1975).
32. K. Czamara et al., Raman spectroscopy of lipids: A review. *J. Raman Spectrosc.* **46**, 4–20 (2015).
33. C. Otto, T. J. J. van den Tweel, F. F. M. de Mul, J. Greve, Surface-enhanced Raman spectroscopy of DNA bases. *J. Raman Spectrosc.* **17**, 289–298 (1986).
34. T. Matsunaga, T. Mori, O. Nikaido, Base sequence specificity of a monoclonal antibody binding to (6-4)photoproducts. *Mutat. Res.* **235**, 187–194 (1990).
35. J. S. Singh, FTIR and Raman spectra and fundamental frequencies of biomolecule: 5-methyluracil (thymine). *J. Mol. Struct.* **876**, 127–133 (2008).
36. K. Szczepaniak, M. M. Szczesniak, W. B. Person, Raman and infrared spectra of thymine. A matrix isolation and DFT study. *J. Phys. Chem. A* **104**, 3852–3863 (2000).
37. S. L. Zhang, K. H. Michaelian, G. R. Loppnow, Vibrational spectra and experimental assignments of thymine and nine of its isotopomers. *J. Phys. Chem. A* **102**, 461–470 (1998).
38. B. Prescott, W. Steinmetz, G. J. Thomas Jr, Characterization of DNA structures by laser Raman spectroscopy. *Biopolymers* **23**, 235–256 (1984).
39. F. D'Amico et al., Oxidative damage in DNA bases revealed by UV resonant Raman spectroscopy. *Analyst (Lond.)* **140**, 1477–1485 (2015).